BUCOURT, R. & HAINAUT, D. (1965). *Bull. Soc. Chim. Fr.* pp. 1366–1378.

DE TITTA, G. T., EDMONDS, J. W., LANGS, D. A. & HAUPTMAN, H. (1975). *Acta Cryst.* A31, 472–479.

DUAX, W. L. & NORTON, D. A. (1975). *Atlas of Steroid Structure.* London: Plenum.

GEISE, H. J., BUYS, H. R. & MIJLHOFF, F. C. (1971). *J. Mol. Struct.* **9**, 447–452.

GRAAFF, R. A. G. DE & ROMERS, C. (1974). *Acta Cryst.* B30, 2029–2033.

GUY, J. J., ALLEN, F. H., KENNARD, O. & SHELDRICK, G. M. (1977). *Acta Cryst.* B33, 1236–1244.

JONES, P. G., FALVELLO, L. & KENNARD, O. (1978). *Acta Cryst.* B34, 1939–1942.

POTENZA, J., MASTROPAOLO, D., GALLAHER, D. & HENDERSON, T. (1975). *Acta Cryst.* B31, 1975–1977.

ROBERTS, P. J., PETTERSEN, R. C., SHELDRICK, G. M., ISAACS, N. W. & KENNARD, O. (1973). *J. Chem. Soc. Perkin Trans.* 2, pp. 1978–1984.

SHELDRICK, G. M. (1977). Private communication.

SHELDRICK, G. M. (1978). In *Direct Methods of Solving Crystal Structures.* International School of Crystallography, Erice, Italy.

TAYLOR, I. F., WATSON, W. H. & SMITH, W. B. (1976). *Cryst. Struct. Commun.* **5**, 883–890.

WARNER, P. M., LU, S.-L., MYERS, E., DEHAVEN, P. W. & JACOBSON, R. A. (1977). *J. Am. Chem. Soc.* **99**, 5102–5108.

WHITE, P. S. & WOOLFSON, M. M. (1975). *Acta Cryst.* A31, 53–56.

Acta Cryst. (1979). B35, 2126–2135

Neutron Diffraction Study of Quinolinic Acid Recrystallized from D_2O: Evaluation of Temperature and Isotope Effects in the Structure*

BY FUSAO TAKUSAGAWA AND THOMAS F. KOETZLE†

Chemistry Department, Brookhaven National Laboratory, Upton, New York 11973, *USA*

(*Received* 15 *February* 1979; *accepted* 15 *May* 1979)

Abstract

The structure of quinolinic acid recrystallized from D_2O (2,3-pyridinedicarboxylic acid; $C_7H_3D_2NO_4$) has been refined based on neutron diffraction data measured at four temperatures: 35, 80, 100 and 298 K. The principal temperature dependence in cell constants is observed for the *b* axis, which is perpendicular to the molecular planes. The refined thermal parameters have been extrapolated by a least-squares procedure, to yield values for $T = 0$ K which provide estimates of the combined effects of static disorder and zero-point motion. The D atom shifts toward the midpoint of the short intramolecular O···O hydrogen bond when the crystal is cooled, just as was found in an earlier study to occur for the H atom in the undeuterated material. At 100 and 298 K, the D atom is displaced significantly further from the bond midpoint than is the H atom at the same temperature. The magnitude of this isotope effect appears to be independent of temperature. The exchangeable protons in the crystal have not been completely replaced by D; refinement of the D scattering lengths indicates the presence of approximately 2·7% H attached to N(1) and 4·4% H in the short hydrogen bond. The N scattering length has been refined to yield a value of 0·921 (2) × 10^{-11} mm.

Introduction

The general features of the crystal structure of quinolinic acid with a very short asymmetric intramolecular hydrogen bond have been elucidated from X-ray photographic data by Takusagawa, Hirotsu & Shimada (1973). Positions of the H atoms, including that in the short hydrogen bond, O···O 2·398 (3) Å, have been confirmed by neutron diffraction techniques at room temperature by Kvick, Koetzle, Thomas & Takusagawa (1974). Recently we have studied effects of temperature on the crystal structure (Takusagawa & Koetzle, 1978) and have observed a shift of the H atom toward the midpoint of the O···O hydrogen bond upon cooling the crystal to 100 K. We have now refined the structure of quinolinic acid based on neutron diffraction data collected with a sample recrystallized from D_2O. Measurements were made at 35, 80, 100 and 298 K, in an attempt to confirm the temperature effects observed in the undeuterated material and in order to elucidate the relationship between temperature and the

* Research carried out at Brookhaven National Laboratory under contract with the US Department of Energy and supported by its Division of Basic Energy Sciences.

† To whom correspondence should be addressed.

effects of D substitution. This work is part of a study of charge-density distributions in quinolinic acid by a combination of X-ray and neutron diffraction techniques.

Experimental section and data reduction

The sample of quinolinic acid used in this work was recrystallized three times from D_2O. The monoclinic crystal had a volume of 7·9 mm³ and was mounted on an aluminum pin along the crystallographic [10$\bar{3}$] direction. It was sealed in an aluminum can filled with helium gas.* The can was placed in a closed-cycle helium refrigerator (Air Products and Chemicals, Inc.; DISPLEX® Model CS-202) and mounted on an automated four-circle diffractometer (Dimmler, Greenlaw, Kelley, Potter, Rankowitz & Stubblefield, 1976; McMullan, Andrews, Koetzle, Reidinger, Thomas & Williams, 1976) at the Brookhaven High Flux Beam Reactor, with a crystal-monochromated neutron beam of wavelength 1·0513 Å (based upon KBr, $a = 6·600$ Å at 298 K). The temperatures recorded during data collection were 35 ± 0·5, 80 ± 0·5, 100 ± 0·5* and 298 ± 3 K. Cell dimensions refined by a least-squares procedure based on setting angles of 29 reflections are listed in Table 1. Intensities were measured for reflections comprising two octants of reciprocal space (hkl, $hk\bar{l}$) and portions of two additional octants ($h\bar{k}l$ and $h\bar{k}\bar{l}$). A $\theta/2\theta$ step-scan technique was employed, with the scan range varied according to $\Delta 2\theta = 1·98° \times (1·0 + 2·98 \tan\theta)$ for the high-angle data ($2\theta \geq 50°$), and $\Delta 2\theta = 4·0°$ for the low-angle data. The step size was adjusted to give approximately 66 points in each scan. As a general check on experimental stability, the intensities of two reflections were remeasured every 100 reflections. These did not vary to any significant degree during the entire period of data collection at any given

* For data collection at room temperature (298 K), the crystal was sealed in a glass capillary and mounted directly on the diffractometer.

* Calibration of the refrigerator by observation of the magnetic phase transition in FeF_2 at 78·4 K indicated that the actual sample temperatures are within 2 K of these recorded values.

Table 1. *Crystal data for quinolinic acid*

2,3-Pyridinedicarboxylic acid, $C_7H_3D_2NO_4$ (D-QNA), $M_r = 169·11$, space group $P2_1/c$, $Z = 4$.

Cell constants and linear absorption coefficients

	35 K (D)	80 K (D)	100 K (D)	100 K (H)*	298 K (D)†	298 K (H)‡
a (Å)	7·420 (2)	7·420 (2)	7·422 (2)	7·414 (1)	7·421 (1)	7·422 (1)
b (Å)	12·308 (4)	12·366 (4)	12·392 (4)	12·389 (2)	12·695 (2)	12·705 (2)
c (Å)	7·831 (4)	7·833 (4)	7·835 (5)	7·832 (1)	7·831 (1)	7·834 (1)
β (°)	117·06 (2)	117·06 (2)	117·06 (2)	117·05 (1)	116·96 (2)	116·95 (1)
V (Å³)	636·9 (4)	640·0 (4)	641·7 (4)	640·7 (2)	657·6 (2)	658·5 (2)
μ§ (mm⁻¹)	0·0763	0·0758	0·0755	0·1247	0·0737	0·1227

* By X-rays (Mo $K\alpha_1$, $\lambda = 0·70926$ Å) (Kvick, 1978).
† By X-rays (Cu $K\alpha_1$, $\lambda = 1·5405$ Å).
‡ By X-rays (Cr $K\alpha_1$, $\lambda = 2·2896$ Å) (Kvick *et al.*, 1974).
§ The effective absorption cross section for incoherent scattering of H was taken to be 40 barn (4000 fm²).

Table 2. *Experimental and refinement parameters (conventional refinement with anisotropic thermal parameters)*

Crystal weight	13·5 mg
Crystal volume at room temperature	7·9 mm³
Number of faces	13

	35 K	80 K	100 K	298 K
Number of reflections measured	2415	1745	1747	2735
Agreement factor on averaging (R_c)*	0·015	0·017	0·017	0·031
Number of independent reflections	1694	1533	1534	2191
Range of sin θ/λ (Å⁻¹)	0·0 ~ 0·71	0·0 ~ 0·66	0·0 ~ 0·66	0·0 ~ 0·73
$R(F^2) = \sum\|F_o^2 - k^2F_c^2\|/\sum F_o^2$	0·032	0·032	0·032	0·046
$wR(F^2) = (\sum w\|F_o^2 - k^2F_c^2\|/\sum wF_o^4)^{1/2}$	0·053	0·053	0·054	0·085
S† $= [\sum w\|F_o^2 - k^2F_c^2\|^2/(m-n)]^{1/2}$	1·55	1·50	1·54	1·83

* $R_c = \sum\left(\sum_{i=1}^{n'} |\langle F_o^2\rangle - F_{o_i}^2|\right)/\sum n'\langle F_o^2\rangle$; n' is the number of equivalent observations for a given reflection.

† m is the number of reflections and n is the number of variable parameters (158).

temperature. Experimental quantities of interest are listed in Table 2 along with some details of the subsequent refinements.

Integrated intensities of reflections were obtained by a method described earlier (Takusagawa & Koetzle, 1978). Absorption corrections for observed intensities were calculated by a modification of the analytical method of de Meulenaer & Tompa (1965) (Alcock, 1970; Templeton & Templeton, 1973). The variance of the net intensity of each reflection was estimated as follows: $\sigma^2(I) = \bar{T} + \bar{B} + [0{\cdot}03(T-B)]^2 + (0{\cdot}03B)^2 + C$, where T and B are total and background counts, respectively, and the factor 0·03 represents an estimate of non-Poisson errors. The constant C was adjusted to yield a uniform value of $\langle \Delta F^2/\sigma(F^2)\rangle$ in all regions of F^2 upon completion of the refinements. Final values of C on an absolute scale in units of 10^{-22} mm^2 are 5·6 (35 K), 4·7 (80 K), 4·1 (100 K) and 0·0 (298 K). Squared observed structure factors were obtained as $F_o^2 = I \times \sin 2\theta$ and averaged for symmetry-related reflections (agreement factors are included in Table 2).

Structure refinement

The atomic coordinates from the neutron diffraction study of Takusagawa & Koetzle (1978) were used as initial values for a full-matrix least-squares refinement minimizing $\sum w(F_o^2 - k^2F_c^2)$ and using a modification of the program by Busing, Martin & Levy (1962). Weights were chosen as $w = 1/\sigma^2(F^2) = 1/[\sigma^2(I) \times \sin^2 2\theta]$. Positional and anisotropic thermal parameters were varied for all atoms together with a scale factor, k, the coherent neutron scattering length of D and N atoms, and a type (I) isotropic extinction correction parameter (Becker & Coppens, 1975). A correction was applied for the effects of a small number of neutrons in the incident beam with wavelength $\lambda/2$, by means of a least-squares procedure, minimizing $\sum w[(1/k^2)F_o^2(hkl) - F_c^2(hkl) - k'F_c^2(2h2k2l)]^2$. The values of k' obtained are 0·0021 (5) for 35 K, 0·0028 (5) for 80 K, 0·0031 (5) for 100 K and 0·0019 (5) for 298 K. Final positional and thermal parameters obtained from refinements performed after correction for the $\lambda/2$ component are listed in Table 3.*

Rigid-body analyses, the results of which will be discussed below in some detail, indicate large librational motions around the C–C bonds of the carboxyl groups. Therefore, in order to investigate the possible significance of curvilinear or anharmonic motion, third- and fourth-order thermal tensors for the four O atoms and the D in the intramolecular hydrogen bond were refined using the expansion developed by Johnson (1970*a*,*b*). A summary of these refinements is given in Table 4. Based on the R-value test (Hamilton, 1965), the fit of the model to the observed data was judged to be improved significantly only for the 298 K study. In any event, the positional parameters were essentially identical to those obtained in the conventional refinements. Neutron scattering lengths used (all × 10^{-11} mm) are $b_C = 0{\cdot}665$ (Bacon, 1972), $b_H = -0{\cdot}374$, $b_O = 0{\cdot}580$, $b_D = 0{\cdot}6672$ (Shull, 1972), and $b_N = 0{\cdot}921$ (2). As noted above, the value for N was refined, along with the effective scattering length for D which was used as a measure of the extent of deuteration.

Discussion

The general features of the structure have been treated in detail in earlier papers (Takusagawa *et al.*, 1973; Kvick *et al.*, 1974). The present discussion will mainly be restricted to those aspects of the structure which are observed to change with temperature, and the effects of

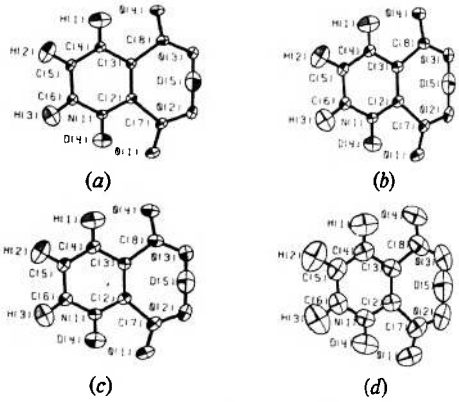

Fig. 1. Molecular views of D-QNA at (*a*) 35 K, (*b*) 80 K, (*c*) 100 K, and (*d*) 298 K. Thermal ellipsoids are drawn at the 97% probability level.

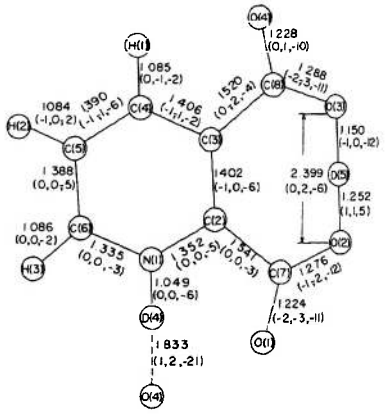

Fig. 2. Bond distances (Å) at 35 K. The differences, $\Delta D(T) = D(T) - D(35)$, for T = 80, 100, and 298 K, respectively, are given in parentheses below the values at 35 K. Estimated standard deviations are 0·002 ~ 0·003 Å.

* Lists of structure factors obtained at 35, 80, 100 and 298 K have been deposited with the British Library Lending Division as Supplementary Publication No. SUP 34465 (42 pp.). Copies may be obtained through The Executive Secretary, International Union of Crystallography, 5 Abbey Square, Chester CH1 2HU, England.

Table 3. *Positional and thermal parameters from the conventional refinement*

Thermal parameters are of the form $\exp[-2\pi^2(h^2a^{*2}U_{11} + \ldots + 2hka^*b^*U_{12} + \ldots)]$.

	x	y	z	U_{11}	U_{22}	U_{33}	U_{12}	U_{13}	U_{23}
N(1)298 K	0·93600 (8)	0·12237 (6)	0·10547 (8)	0·0154 (3)	0·0440 (4)	0·0199 (3)	0·0011 (2)	0·0103 (2)	0·0006 (2)
100	0·93732 (7)	0·12241 (4)	0·10789 (6)	0·0071 (2)	0·0142 (3)	0·0072 (2)	0·0003 (2)	0·0043 (2)	−0·0001 (1)
80	0·93747 (7)	0·12242 (4)	0·10803 (6)	0·0063 (2)	0·0122 (2)	0·0060 (2)	0·0004 (2)	0·0037 (2)	0·0001 (1)
35	0·93772 (6)	0·12241 (3)	0·10840 (6)	0·0047 (2)	0·0084 (2)	0·0042 (2)	0·0002 (1)	0·0026 (2)	−0·0001 (1)
C(2)298	0·7342 (1)	0·12462 (7)	−0·0042 (1)	0·0167 (3)	0·0337 (4)	0·0159 (3)	0·0005 (3)	0·0089 (2)	0·0002 (3)
100	0·73464 (9)	0·12461 (5)	−0·00241 (8)	0·0081 (3)	0·0115 (3)	0·0063 (2)	0·0004 (2)	0·0039 (2)	0·0004 (2)
80	0·73477 (9)	0·12458 (5)	−0·00221 (9)	0·0073 (3)	0·0100 (3)	0·0054 (2)	0·0000 (2)	0·0034 (2)	0·0001 (2)
35	0·73495 (8)	0·12459 (5)	−0·00198 (8)	0·0052 (2)	0·0071 (2)	0·0039 (2)	0·0004 (2)	0·0024 (2)	0·0005 (2)
C(3)298	0·6111 (1)	0·12623 (7)	0·0877 (1)	0·0143 (3)	0·0331 (4)	0·0180 (3)	0·0001 (3)	0·0087 (2)	−0·0001 (3)
100	0·61138 (9)	0·12623 (5)	0·09003 (8)	0·0067 (3)	0·0113 (3)	0·0069 (3)	0·0001 (2)	0·0034 (2)	−0·0003 (2)
80	0·61162 (9)	0·12624 (5)	0·09027 (8)	0·0065 (3)	0·0098 (3)	0·0061 (3)	0·0002 (2)	0·0033 (2)	−0·0002 (2)
35	0·61169 (8)	0·12620 (5)	0·09055 (8)	0·0043 (2)	0·0072 (2)	0·0039 (2)	0·0001 (2)	0·0018 (2)	−0·0002 (2)
C(4)298	0·7051 (1)	0·12251 (8)	0·2887 (1)	0·0211 (3)	0·0430 (5)	0·0181 (3)	0·0004 (3)	0·0112 (3)	0·0001 (3)
100	0·7058 (1)	0·12212 (5)	0·29122 (8)	0·0092 (3)	0·0140 (3)	0·0070 (3)	−0·0000 (2)	0·0045 (2)	−0·0001 (2)
80	0·7060 (1)	0·12210 (5)	0·29154 (8)	0·0082 (3)	0·0119 (3)	0·0061 (3)	0·0001 (2)	0·0039 (2)	0·0001 (2)
35	0·70630 (8)	0·12197 (5)	0·29201 (8)	0·0053 (2)	0·0085 (2)	0·0043 (3)	−0·0001 (2)	0·0024 (2)	0·0000 (2)
C(5)298	0·9135 (1)	0·12139 (9)	0·3942 (1)	0·0220 (3)	0·0505 (5)	0·0163 (3)	0·0018 (4)	0·0081 (3)	0·0009 (4)
100	0·9151 (1)	0·12134 (5)	0·39742 (9)	0·0090 (3)	0·0165 (3)	0·0060 (3)	0·0007 (2)	0·0033 (2)	0·0006 (2)
80	0·9153 (1)	0·12134 (5)	0·39778 (9)	0·0082 (3)	0·0139 (3)	0·0050 (3)	0·0008 (2)	0·0028 (2)	0·0005 (2)
35	0·91572 (9)	0·12129 (5)	0·39833 (8)	0·0058 (2)	0·0098 (2)	0·0032 (2)	0·0003 (2)	0·0017 (2)	0·0004 (2)
C(6)298	1·0286 (1)	0·12201 (9)	0·2963 (1)	0·0168 (3)	0·0504 (5)	0·0198 (3)	0·0015 (3)	0·0069 (3)	0·0009 (4)
100	1·0306 (1)	0·12201 (6)	0·29923 (9)	0·0083 (3)	0·0166 (3)	0·0071 (3)	0·0005 (2)	0·0036 (2)	0·0003 (2)
80	1·0307 (1)	0·12208 (6)	0·29939 (9)	0·0076 (3)	0·0141 (3)	0·0060 (3)	0·0006 (2)	0·0031 (2)	0·0003 (2)
35	1·03101 (8)	0·12212 (5)	0·29987 (8)	0·0057 (2)	0·0097 (3)	0·0043 (3)	0·0004 (2)	0·0023 (2)	0·0002 (2)
C(7)298	0·6816 (1)	0·12152 (9)	−0·2181 (1)	0·0248 (4)	0·0460 (5)	0·0174 (3)	−0·0011 (3)	0·0117 (3)	−0·0004 (3)
100	0·6820 (1)	0·12101 (5)	−0·21659 (8)	0·0103 (3)	0·0155 (3)	0·0064 (2)	−0·0001 (2)	0·0041 (2)	0·0001 (2)
80	0·6820 (1)	0·12103 (5)	−0·21652 (8)	0·0090 (3)	0·0128 (3)	0·0059 (2)	−0·0002 (2)	0·0038 (2)	−0·0000 (2)
35	0·68206 (9)	0·12094 (5)	−0·21636 (8)	0·0062 (2)	0·0083 (2)	0·0041 (2)	−0·0000 (2)	0·0027 (2)	0·0000 (2)
C(8)298	0·3823 (1)	0·13305 (8)	−0·0064 (1)	0·0158 (3)	0·0416 (5)	0·0266 (4)	−0·0009 (3)	0·0109 (3)	−0·0018 (3)
100	0·38224 (9)	0·13385 (5)	−0·00448 (9)	0·0081 (3)	0·0136 (3)	0·0093 (3)	−0·0004 (2)	0·0052 (2)	−0·0002 (2)
80	0·38217 (9)	0·13393 (5)	−0·00430 (9)	0·0072 (3)	0·0115 (3)	0·0078 (3)	−0·0004 (2)	0·0045 (2)	−0·0006 (2)
35	0·38227 (8)	0·13412 (5)	−0·00387 (8)	0·0055 (2)	0·0076 (2)	0·0054 (3)	−0·0004 (2)	0·0033 (2)	−0·0003 (2)
O(1)298	0·8228 (2)	0·1080 (1)	−0·2538 (2)	0·0345 (6)	0·088 (1)	0·0254 (5)	0·0019 (6)	0·0213 (4)	−0·0008 (6)
100	0·8240 (1)	0·10685 (7)	−0·2525 (1)	0·0138 (3)	0·0271 (4)	0·0094 (3)	0·0006 (3)	0·0079 (3)	−0·0002 (3)
80	0·8241 (1)	0·10682 (7)	−0·2525 (1)	0·0120 (3)	0·0226 (4)	0·0081 (3)	0·0006 (3)	0·0067 (2)	−0·0002 (3)
35	0·8245 (1)	0·10664 (6)	−0·2523 (1)	0·0081 (3)	0·0148 (3)	0·0061 (3)	0·0007 (2)	0·0046 (2)	0·0001 (2)
O(2)298	0·4993 (2)	0·1354 (1)	−0·3394 (1)	0·0281 (5)	0·079 (1)	0·0173 (4)	0·0026 (5)	0·0065 (4)	0·0042 (5)
100	0·4980 (1)	0·13498 (7)	−0·3390 (1)	0·0114 (4)	0·0250 (4)	0·0066 (3)	0·0009 (3)	0·0026 (3)	0·0012 (3)
80	0·4977 (1)	0·13487 (7)	−0·3389 (1)	0·0103 (3)	0·0204 (4)	0·0056 (3)	0·0008 (3)	0·0025 (3)	0·0010 (3)
35	0·4976 (1)	0·13487 (6)	−0·3388 (1)	0·0066 (3)	0·0135 (3)	0·0042 (3)	0·0006 (2)	0·0018 (2)	0·0005 (2)
O(3)298	0·2863 (2)	0·1528 (1)	−0·1855 (2)	0·0175 (4)	0·093 (1)	0·0284 (5)	0·0034 (5)	0·0059 (4)	0·0078 (6)
100	0·2853 (1)	0·15540 (7)	−0·1843 (1)	0·0086 (3)	0·0296 (4)	0·0094 (3)	0·0010 (3)	0·0032 (3)	0·0023 (3)
80	0·2852 (1)	0·15557 (7)	−0·1842 (1)	0·0079 (3)	0·0245 (4)	0·0078 (3)	0·0012 (3)	0·0029 (3)	0·0021 (3)
35	0·2853 (1)	0·15600 (6)	−0·1841 (1)	0·0057 (3)	0·0157 (3)	0·0051 (3)	0·0007 (2)	0·0023 (2)	0·0012 (2)
O(4)298	0·2983 (2)	0·1198 (1)	0·0943 (2)	0·0210 (4)	0·0755 (9)	0·0365 (5)	−0·0017 (5)	0·0192 (4)	0·0004 (6)
100	0·2979 (1)	0·12010 (7)	0·0973 (1)	0·0095 (3)	0·0241 (4)	0·0125 (3)	−0·0011 (3)	0·0072 (3)	0·0002 (3)
80	0·2980 (1)	0·12007 (7)	0·0975 (1)	0·0088 (3)	0·0198 (4)	0·0105 (3)	−0·0007 (3)	0·0063 (2)	0·0004 (3)
35	0·2982 (1)	0·12018 (6)	0·0980 (1)	0·0063 (3)	0·0131 (3)	0·0068 (3)	−0·0005 (2)	0·0043 (2)	0·0005 (2)
H(1)298	0·6109 (3)	0·1214 (2)	0·3612 (3)	0·0373 (9)	0·088 (2)	0·0359 (9)	0·002 (1)	0·0251 (8)	0·001 (1)
100	0·6120 (2)	0·1207 (1)	0·3641 (2)	0·0229 (7)	0·0408 (8)	0·0208 (6)	0·0004 (6)	0·0153 (5)	0·0001 (6)
80	0·6122 (2)	0·1206 (1)	0·3647 (2)	0·0220 (7)	0·0387 (8)	0·0199 (6)	0·0004 (6)	0·0148 (5)	−0·0001 (6)
35	0·6123 (2)	0·1204 (1)	0·3650 (2)	0·0184 (5)	0·0337 (7)	0·0178 (6)	0·0002 (5)	0·0129 (5)	−0·0001 (5)
H(2)298	0·9844 (3)	0·1202 (3)	0·5492 (3)	0·041 (1)	0·092 (2)	0·0222 (7)	0·005 (1)	0·0102 (7)	0·002 (1)
100	0·9862 (2)	0·1201 (1)	0·5527 (2)	0·0247 (7)	0·0421 (8)	0·0118 (6)	0·0016 (6)	0·0064 (5)	0·0014 (6)
80	0·9864 (2)	0·1202 (1)	0·5530 (2)	0·0230 (7)	0·0389 (8)	0·0112 (6)	0·0014 (6)	0·0063 (5)	0·0011 (6)
35	0·9869 (2)	0·1205 (1)	0·5537 (2)	0·0198 (6)	0·0328 (7)	0·0090 (5)	0·0017 (5)	0·0049 (5)	0·0013 (5)
H(3)298	1·1921 (3)	0·1210 (3)	0·3644 (3)	0·0222 (8)	0·097 (2)	0·0376 (9)	0·002 (1)	0·0082 (7)	0·001 (1)
100	1·1945 (2)	0·1213 (1)	0·3670 (2)	0·0151 (6)	0·0443 (9)	0·0206 (6)	0·0006 (6)	0·0056 (5)	0·0012 (6)
80	1·1950 (2)	0·1213 (1)	0·3674 (2)	0·0146 (6)	0·0402 (8)	0·0197 (6)	0·0003 (6)	0·0057 (5)	0·0008 (6)
35	1·1954 (2)	0·1213 (1)	0·3676 (2)	0·0117 (5)	0·0338 (7)	0·0171 (6)	0·0002 (5)	0·0049 (4)	0·0008 (5)
D(4)298	1·0266 (2)	0·1204 (1)	0·0354 (2)	0·0269 (5)	0·0628 (8)	0·0359 (6)	0·0019 (4)	0·0213 (4)	0·0009 (5)
100	1·0285 (1)	0·12048 (7)	0·0375 (1)	0·0151 (4)	0·0279 (5)	0·0176 (4)	0·0007 (3)	0·0107 (3)	0·0007 (3)
80	1·0287 (1)	0·12045 (7)	0·0378 (1)	0·0144 (4)	0·0243 (4)	0·0166 (4)	0·0007 (3)	0·0102 (3)	0·0005 (3)
35	1·0289 (1)	0·12045 (6)	0·0381 (1)	0·0126 (3)	0·0199 (4)	0·0136 (4)	0·0007 (2)	0·0085 (3)	0·0006 (3)
D(5)298	0·3861 (2)	0·1483 (1)	−0·2609 (2)	0·0299 (6)	0·088 (1)	0·0288 (6)	0·0005 (6)	0·0049 (4)	0·0079 (6)
100	0·3862 (1)	0·14958 (8)	−0·2601 (1)	0·0166 (4)	0·0331 (5)	0·0153 (4)	0·0005 (3)	0·0036 (3)	0·0030 (3)
80	0·3860 (1)	0·14981 (8)	−0·2601 (1)	0·0156 (4)	0·0289 (5)	0·0136 (4)	0·0007 (3)	0·0033 (3)	0·0029 (3)
35	0·3861 (1)	0·15004 (7)	−0·2599 (1)	0·0128 (4)	0·0213 (4)	0·0116 (4)	0·0004 (3)	0·0028 (3)	0·0021 (3)

D substitution upon the geometry of the hydrogen bonds.

The molecular structure of D-QNA* in the crystalline state at 35, 80, 100 and 298 K is illustrated in Fig. 1 (Johnson, 1976), and bond distances and angles are shown in Figs. 2 and 3 respectively. Differences in bond distances between D-QNA and H-QNA (Kvick *et al.*, 1974; Takusagawa & Koetzle, 1978) are presented in Fig. 4

Temperature effects in D-QNA

The effects of cooling on the structure are very similar to those observed in H-QNA (Takusagawa & Koetzle, 1978). The principal change in cell dimensions is observed for the crystallographic *b* axis, which is perpendicular to the molecular planes (refer to Table 1). There is no hydrogen bonding between these molecular sheets (Takusagawa *et al.*, 1973; Kvick *et al.*, 1974), which interact only by means of van der Waals forces. No significant change with temperature is observed in the *a* and *c* axes, *i.e.* within molecular sheets. The relationship between temperature and the length of the *b* axis for D-QNA is quite linear, as illustrated in Fig. 5. The calculated linear-expansion coefficient, β, is $1{\cdot}19 \times 10^{-4}$ K^{-1}. Results of rigid-body thermal-motion analyses carried out by the method of Schomaker & Trueblood (1968) are summarized in Table 5 and indicate that the largest translational tensor component at 298 K is perpendicular to the molecular planes (T_Z). **S** tensor components were in all cases quite small: the largest effective screw translation is calculated to be 0·006 Å. All translational and librational tensor components are markedly reduced when the crystal is cooled, as expected. In particular, the large decrease in T_Z together with that in L_X and L_Y, and the resulting decrease in amplitude of out-of-plane motion allows shorter van der Waals contacts between the molecular planes and is in turn related to the decrease in the *b*-axis repeat.

* The notation D-QNA and H-QNA will be used here to indicate respectively quinolinic acid recrystallized from D_2O, and ordinary undeuterated quinolinic acid.

Table 4. *Summary of refinements incorporating third- and fourth-order thermal tensors for* O(1), O(2), O(3), O(4) *and* D(5)

		$wR(F^2)$			
Temperature	m	(I)*	(II)†	(III)‡	(IV)§
35 K	1694	0·053	0·051	—	0·053 (159)
80	1533	0·053	0·051	—	0·052 (161)
100	1534	0·054	0·053	—	0·053 (163)
298	2191	0·085	0·081	0·080	0·083 (163)

* Conventional refinement, with second-order thermal tensors ($n = 158$).

† Refinement including third-order thermal tensors ($n = 208$).

‡ Refinement including third- and fourth-order thermal tensors ($n = 283$). Fourth-order coefficients did not converge owing to very high correlations with second-order terms, except for the 298 K data.

§ Refinements in which the values of all third- and fourth-order coefficients having magnitudes less than 3σ have been set equal to 0 (n given in parentheses).

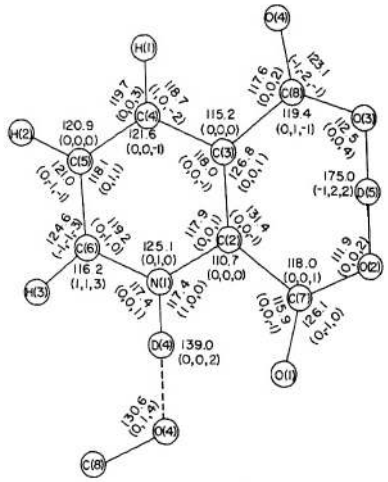

Fig. 3. Bond angles (°) at 35 K. The differences, $\Delta A(T) = A(T) - A(35)$, for T = 80, 100 and 298 K, respectively, are given in parentheses below the values at 35 K. Estimated standard deviations are 0·1° except 0·1 ~ 0·2° for O(2)–D(5)–O(3).

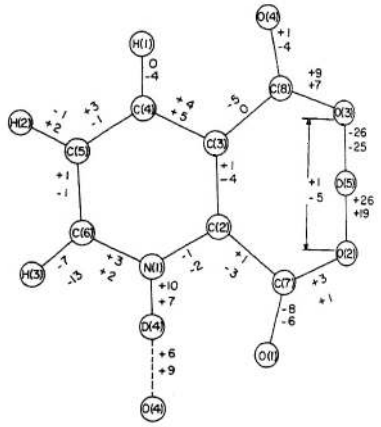

Fig. 4. Isotope effects on bond distances at 100 and 298 K. The values shown are Diff. (100 K) = D(100 K) − H(100 K) and Diff. (298 K) = D(298 K) − H(298 K). The value at 100 K is shown above that at 298 K. Units are 0·001 Å.

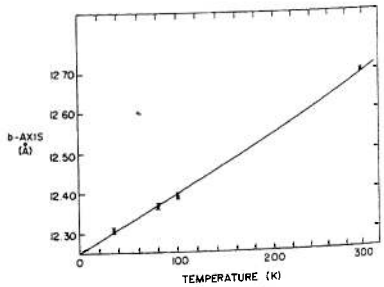

Fig. 5. Relationship between temperature and the length of the *b* axis.

Fig. 6 displays difference thermal ellipsoids calculated as U_{ij} (Diff.) = U_{ij} (T_1) − U_{ij} (T_2), which show the reduction of thermal motion for each atom between temperatures T_1 and T_2. These difference thermal motions apparently are quite reasonable for all atoms. Fig. 7 shows the relationship between temperature and the magnitude of each of the six U_{ij} classes, which seems to be quite linear in the low-temperature region. From Fig. 7, it is apparent that U_{22}, U_{12} and U_{23} classes which are related to motions perpendicular to the molecular plane are more reduced at low temperature than are U_{11}, U_{33} and U_{13} which represent motions in the molecular plane. Using the slopes for each U_{ij} class from Fig. 7, it is possible to extrapolate U values for $T = 0$ K. These values are 79·3, 72·5, 78·1, 85·7, 78·7 and 67·4% of U_{ij} at 35 K for U_{11}, U_{22}, U_{33}, U_{12}, U_{13}, and U_{23} respectively. A second procedure was used to extrapolate the thermal parameters to 0 K using individual second-order polynomials to represent U_{ij} for each atom as a function of temperature, with the three coefficients determined by a least-squares procedure. Extrapolated U_{ij} values at 0 K obtained in this fashion are listed in Table 6 and the corresponding ellipsoids are drawn in Fig. 8. These parameters provide estimates of the combined effects of zero-point motion and static disorder. The U_{ij} ($T = 0$ K) values in Table 6 have been subjected to rigid-body thermal-motion analyses, and results of these calculations are included in Table 5.

The observed differences in bond distances with temperature (Fig. 2) are quite easily explained in terms of foreshortening due to rigid-body libration, except in the case of the intramolecular hydrogen bond. Estimates of the average magnitudes of these corrections for

Table 5. *Summary of rigid-body thermal-motion analyses*

The units for mean-square amplitude of translational vibration (**T**), libration vibration (**L**), and root-mean-square fit $\langle \Delta U^2 \rangle^{1/2}$ are 0·0001 Å^2, 0·0001 rad^2 and 0·0001 Å^2 respectively.

Model*	Temperature	T_X	T_Y	T_Z	L_X	L_Y	L_Z	$\langle \Delta U^2 \rangle^{1/2}$
(1) 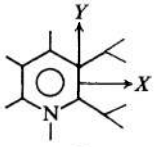	298 K	181	137	250	63	64	24	41
	100	83	59	64	27	26	11	30
	80	76	52	49	25	23	10	30
	35	57	37	22	21	18	8	30
	0	44	25	3	18	15	6	30
(2) 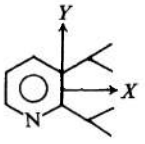	298	169	132	257	52	63	20	31
	100	73	57	91	15	19	6	10
	80	64	52	80	12	15	5	8
	35	46	38	59	7	9	3	6
	0	32	29	46	4	4	2	5
(3) 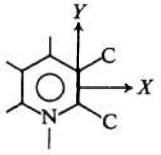	298	180	135	227	74	44	28	32
	100	84	56	33	44	23	15	27
	80	77	50	18	42	21	14	28
	35	57	37	−9	38	18	12	27
	0	43	27	−28	36	15	11	28
(4) 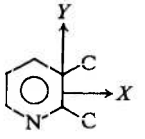	298	167	134	316	38	24	20	4
	100	72	58	110	10	8	5	3
	80	63	53	96	7	6	4	3
	35	44	39	70	3	3	3	2
	0	30	30	52	0	0	2	3
(5) 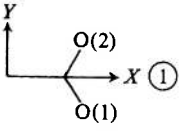	298	154	160	337	226	52	32	6
	100	59	77	115	59	17	11	2
	80	52	69	100	52	12	9	2
	35	39	49	72	40	5	5	2
	0	31	34	54	37	−1	3	3
(6) 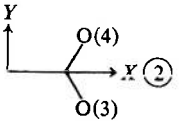	298	151	169	332	296	35	29	8
	100	76	59	113	91	10	9	4
	80	71	50	98	76	7	7	3
	35	52	34	72	53	2	4	3
	0	38	24	57	39	−2	2	3

* Coordinate systems used in these calculations are indicated by the arrows → X and → Y. The Z coordinate is taken in the direction perpendicular to the page. For models (1)–(4), the **S** tensor was included in the calculations, and the results transformed to place the origin at the center of reaction. For models (5) and (6), the origin was fixed at the ring C atom, and the **S** tensor was not included.

distances are given in Table 7. No significant changes are found for bond angles.

Displacements from the least-squares plane through the six non-hydrogen atoms of the pyridine ring are shown in Fig. 9. Significant changes in these displacements with temperature are observed for the carboxyl groups, where the librations around the C–C bonds are very much reduced when the crystal is cooled, as can be seen from the L_X values for these groups given in Table 5.

When the D-QNA crystal is cooled to 100 K or below, the intramolecular hydrogen-bond distance O(2)···O(3) increases very slightly (0·006–0·008 Å), and D(5) moves approximately 0·008 Å closer to the midpoint of the hydrogen bond, compared to the structure at 298 K. In the N(1)–D(4)···O(4)–C(8) hydrogen bond, there is a slight but possibly significant contraction of 0·02 Å in the D(4)···O(4) distance upon cooling to 100 K or below (Fig. 2). However, part of this change can be traced to the foreshortening of the N(1)–D(4) and O(4)–C(8) bond distances at 298 K, which is adequately accounted for by the effects of rigid-body libration.

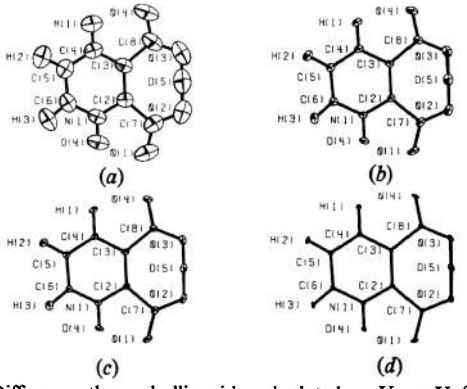

Fig. 6. Difference thermal ellipsoids calculated as $U_{ij} = U_{ij}(T_1) - U_{ij}(T_2)$. (*a*) $T_1 = 298$ K, $T_2 = 35$ K, (*b*) $T_1 = 100$ K, $T_2 = 35$ K, (*c*) $T_1 = 80$ K, $T_2 = 35$ K and (*d*) $T_1 = 100$ K, $T_2 = 80$ K. Ellipsoids are drawn as in Fig. 1.

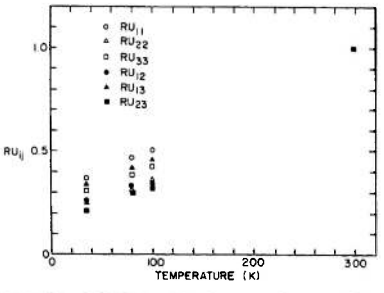

Fig. 7. Relationship between the temperature and average magnitude of each U_{ij} class. $RU_{ij}(T)$ is calculated as follows: $RU_{ij}(T) = \sum U_{ij}(T)U_{ij}(298)/\sum U_{ij}(298)^2$.

Isotope effects

As can be seen by inspection of Table 1, the cell dimensions of H-QNA and D-QNA at both 100 and 298 K are very similar. Possibly significant differences are found in the *a* axis (0·008 Å) at 100 K and the *b* axis (0·010 Å) at 298 K. The differences in bond distances between D-QNA and H-QNA are shown in

Table 6. *Extrapolated U_{ij} values at $T = 0$ K calculated as a second-order polynomial function of temperature (T): $U_{ij}(T) = aT^2 + bT + c$*

Individual coefficients *a*, *b* and *c* for each atom were fitted by a least squares procedure using U_{ij} values at the four different temperatures. For all atoms, the magnitude of *a* is of the order of one per cent that of *b*, or less.

	U_{11}	U_{22}	U_{33}	U_{12}	U_{13}	U_{23}
N(1)	0·0034	0·0061	0·0029	0·0002	0·0018	0·0000
C(2)	0·0036	0·0054	0·0028	0·0005	0·0016	0·0005
C(3)	0·0030	0·0057	0·0024	0·0001	0·0010	−0·0001
C(4)	0·0031	0·0064	0·0031	−0·0001	0·0013	0·0001
C(5)	0·0043	0·0071	0·0019	0·0001	0·0009	0·0002
C(6)	0·0042	0·0068	0·0031	0·0003	0·0016	0·0002
C(7)	0·0042	0·0051	0·0031	0·0000	0·0020	−0·0001
C(8)	0·0041	0·0051	0·0037	−0·0003	0·0023	−0·0004
O(1)	0·0052	0·0097	0·0048	0·0008	0·0030	0·0002
O(2)	0·0042	0·0087	0·0032	0·0005	0·0015	0·0002
O(3)	0·0041	0·0096	0·0033	0·0005	0·0018	0·0007
O(4)	0·0047	0·0086	0·0043	−0·0002	0·0029	0·0008
H(1)	0·0159	0·0315	0·0166	0·0061	0·0117	−0·0001
H(2)	0·0172	0·0291	0·0077	0·0021	0·0039	0·0013
H(3)	0·0096	0·0296	0·0156	−0·0001	0·0045	0·0005
D(4)	0·0115	0·0164	0·0117	0·0007	0·0076	0·0005
D(5)	0·0109	0·0163	0·0098	0·0003	0·0022	0·0017

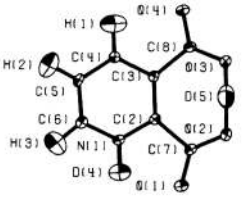

Fig. 8. Extrapolated structure at $T = 0$ K, with ellipsoids drawn as in Fig. 1 and calculated from U_{ij} values given in Table 6.

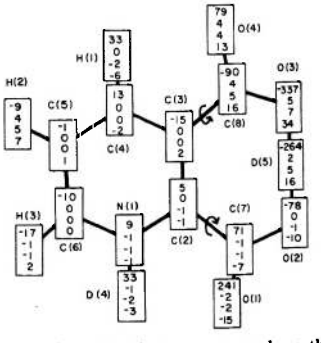

Fig. 9. Displacements from the least-squares plane through the six non-hydrogen atoms of the pyridine ring at 35 K. Changes in displacements (displacement at T − displacement at 35 K) for $T = 80$, 100 and 298 K, respectively, are given below the value at 35 K. Units are 0·001 Å.

Fig. 4. As expected, substantial differences are found in the N(1)–D(4), O(2)–D(5), and O(3)–D(5) bonds. In addition, significant differences are observed for the distances C(7)–O(1), C(8)–O(3) and C(6)–H(3).

A summary of the effects of D substitution on the geometry of the hydrogen bonds is given in Table 8. In the O(2)···D(5)···O(3) system, when the H is replaced by D, it moves approximately 0·025 Å towards O(3). On the other hand, in the N(1)–D(4)···O(4) system, replacement of the H by D causes it to move approximately 0·016 Å in a direction perpendicular to the N(1)···O(4) vector, thus decreasing slightly the N(1)–D(4)···O(4) angle and increasing the N(1)–D(4) and D(4)···O(4) distances. The O(2)···O(3) and N(1)···O(4) distances exhibit no significant change upon deuteration. As can be seen from Fig. 4 and Table 8, the isotope effects observed in this study are found to be independent of temperature, in agreement with the generally accepted interpretation of these effects as a zero-point energy phenomenon (Robertson & Ubbelohde, 1939). A similar conclusion has been reached by Thomas, Tellgren & Olovsson (1974), in an X-ray diffraction study of $KHCO_3$ and $KDCO_3$. This structure exhibits hydrogen-bonded dimers of HCO_3^- ions related by a center of symmetry, and the O···O distances are found to be significantly longer in $KDCO_3$ than in $KHCO_3$. (The magnitude of this effect is 0·022, 0·021, and 0·015 Å at 298, 219 and 95 K respectively.) By contrast, in quinolinic acid the O(2)···O(3) and N(1)···O(4) distances show no significant change upon deuteration. This observation is perhaps not too surprising, since the O(2)···O(3) hydrogen bond is subject to intramolecular constraints, and the N(1)···O(4) bond is of moderate strength. Thomas (1972) has indicated that O···O bonds longer than 2·6 Å may be expected to show no expansion with deuteration, although cooperative effects complicate the situation in crystals exhibiting networks of hydrogen bonds, as noted by Delaplane & Ibers (1969). In ammonium oxalate monohydrate (Taylor & Sabine, 1972) no significant increase in N···O distances was found upon deuteration, for the N–H···O hydrogen bonds.

Systematic differences are observed between the thermal parameters of H-QNA and D-QNA at both 100 and 298 K. However, these differences are reduced to quite small values for all atoms except D(4) and D(5) if the parameters in each U_{ij} class are rescaled using the ratios defined in Table 9. These observed differences in thermal parameters may be caused by a random slipping of the molecular sheets with respect to one another, which might be expected to occur to a different extent in each crystal. This hypothesis is supported by the fact that the ratio for U_{22} is close to 1·0. The differences in thermal parameters of D and H atoms persist even after rescaling, as is reflected in the principal axes of vibration listed in Table 10 and shown graphically in Fig. 10. These differences presumably are caused by the isotopic substitution. In each case the mean-square displacements for D are less than those for H at the same temperature, as one would expect.

Table 7. *Average corrections* (Å) *to bond distances for the effects of rigid-body libration*

Model	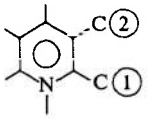	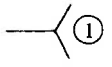	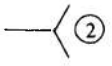
35 K	0·002 ~ 0·003	0·002	0·003
80	0·002 ~ 0·004	0·003	0·004
100	0·003 ~ 0·004	0·003 ~ 0·004	0·005
298	0·005 ~ 0·007	0·013 ~ 0·014	0·015 ~ 0·018

Scattering lengths of N *and* D

The neutron scattering length of N has been refined at each temperature and the values obtained are 0·921 (4), 0·920 (4), 0·919 (4), and 0·922 (4) × 10^{-11} mm at 35, 80, 100 and 298 K respectively. The deviations from the mean value of 0·921 (2) × 10^{-11} mm are within one estimated standard deviation. This result is actually somewhat smaller than the value of

Table 8. *Comparison of the hydrogen-bond geometries in* H-QNA *and* D-QNA *at* 100 *and* 298 K

(*A*) N(1)–H(4)···O(4)–C(8)

	N(1)–H(4)	H(4)···O(4)	O(4)–C(8)	N(1)···O(4)	∠N(1)–H(4)···O(4)	∠H(4)···O(4)–C(8)
100 K (H)	1·039 (3) Å	1·829 (4) Å	1·228 (3) Å	2·710 (3) Å	140·2 (2)°	130·8 (2)°
100 (D)	1·049 (1)	1·835 (1)	1·229 (1)	2·715 (2)	139·0 (1)	130·7 (1)
298 (H)	1·036 (4)	1·845 (4)	1·222 (3)	2·725 (2)	140·5 (2)	131·5 (2)
298 (D)	1·043 (2)	1·854 (2)	1·218 (2)	2·730 (2)	139·2 (1)	131·0 (1)

(*B*) C(7)–O(2)···H(5)···O(3)–C(8)

	O(2)···H(5)	H(5)···O(3)	O(2)···O(3)	∠O(2)···H(5)···O(3)	∠C(7)–O(2)···H(5)	∠H(5)···O(3)–C(8)
100 K (H)	1·227 (3) Å	1·176 (3) Å	2·400 (2) Å	174·5 (2)°	111·8 (2)°	112·4 (2)°
100 (D)	1·253 (2)	1·150 (2)	2·401 (2)	175·2 (1)	111·9 (1)	112·5 (1)
298 (H)	1·238 (5)	1·163 (5)	2·398 (3)	174·4 (4)	111·4 (4)	112·7 (4)
298 (D)	1·257 (2)	1·138 (2)	2·393 (2)	175·2 (2)	112·1 (1)	112·9 (1)

$0{\cdot}936 \times 10^{-11}$ mm recently given by Koester (1977), but agrees well with $0{\cdot}917\ (9) \times 10^{-11}$ mm, an average value taken from several other structure refinements based upon single-crystal data (Kvick *et al.*, 1974). In this context, the value of $0{\cdot}941\ (5) \times 10^{-11}$ mm obtained for H-QNA at 100 K (Takusagawa & Koetzle, 1978) appears to be somewhat larger than normal.

The two D scattering lengths were also allowed to vary in the refinements. The refined values are lower than the normal value of $b_D = 0{\cdot}6672 \times 10^{-11}$ mm

Table 9. *Ratios of thermal parameters of* D-QNA *and* H-QNA

$RU_{ij} = \sum U_{ij}(\mathrm{D})\, U_{ij}(\mathrm{H}) / \sum U_{ij}(\mathrm{H})^2$, where the summation extends over all atoms except H(4) and H(5).

Temperature	RU_{11}	RU_{22}	RU_{33}	RU_{12}	RU_{13}	RU_{23}
100 K	0·9108	0·9822	0·8277	0·7853	0·6675	0·8815
298	0·8286	0·9747	0·8913	0·7452	0·8006	1·0424

Table 10. *Principal axes of vibration for* D *and* H *atoms*

		Mean-square displacement*	Direction cosines† l	m	n
(*a*) 100 K					
U_{11}	H(4)	0·0346	−0·0032	0·9942	0·1076
	D(4)	0·0279	−0·0195	0·9959	0·0883
U_{22}	H(4)	0·0228	0·3588	−0·0993	0·9281
	D(4)	0·0188	−0·1026	−0·0898	0·9907
U_{33}	H(4)	0·0141	0·9334	0·0416	−0·3563
	D(4)	0·0101	0·9945	0·0104	0·1040
U_{11}	H(5)	0·0394	0·4105	0·9103	−0·0540
	D(5)	0·0338	0·2983	0·9484	−0·1075
U_{22}	H(5)	0·0230	0·9118	−0·4092	0·0344
	D(5)	0·0222	0·9543	−0·2946	0·0500
U_{33}	H(5)	0·0200	−0·0092	0·0633	0·9980
	D(5)	0·0131	−0·0138	0·1178	0·9929
(*b*) 298 K					
U_{11}	H(4)	0·0768	−0·0059	0·9946	0·1037
	D(4)	0·0630	0·0344	0·9993	−0·0172
U_{22}	H(4)	0·0413	0·0388	−0·1035	0·9939
	D(4)	0·0375	−0·1955	−0·0569	0·9791
U_{33}	H(4)	0·0204	0·9992	0·0100	−0·0383
	D(4)	0·0170	0·9807	−0·0063	0·1955
U_{11}	H(5)	0·0919	0·2994	0·9524	−0·0571
	D(5)	0·0895	0·2525	0·9639	−0·0847
U_{22}	H(5)	0·0441	0·9489	−0·3033	−0·0871
	D(5)	0·0435	0·9670	−0·2544	−0·0122
U_{33}	H(5)	0·0306	0·1002	0·0280	0·9946
	D(5)	0·0232	0·0332	0·0788	0·9963

* Mean-square displacements are in Å², and those for H atoms have been rescaled using the ratios given in Table 9.

† Defined relative to the following bases: for H,D(4), X_1 is along N(1)–H,D(4), X_2 lies in the *ac* plane and X_3 is normal to X_1 and X_2; for H,D(5), X_1 is along O(2)···O(3), X_2 lies in the *ac* plane and X_3 is normal to X_1 and X_2.

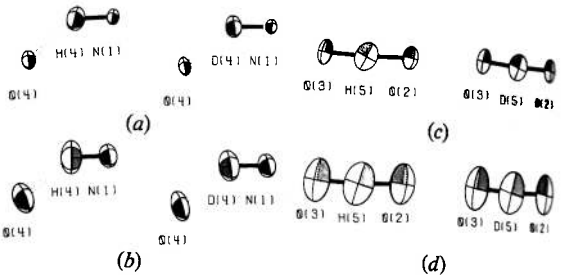

Fig. 10. Comparison of thermal parameters of H-QNA and D-QNA for atoms involved in hydrogen bonds. Values for H-QNA have been rescaled using the ratios given in Table 9. (*a*) N–H···O at 100 K, (*b*) N–H···O at 298 K, (*c*) O···H···O at 100 K, (*d*) O···H···O at 298 K. The direction of view is approximately parallel to the plane of the pyridine ring.

Table 11. *Deuterium scattering lengths* ($\times 10^{-11}$ mm) *and calculated percentage occupancy of protons*

	D(4)		D(5)	
Temperature	Scattering length	H (%)	Scattering length	H (%)
35 K	0·641 (4)	2·6 (4)	0·620 (4)	4·6 (4)
80	0·640 (4)	2·6 (4)	0·619 (4)	4·7 (4)
100	0·641 (4)	2·6 (4)	0·622 (4)	4·4 (4)
298	0·636 (4)	3·0 (3)	0·624 (4)	4·2 (4)

(Shull, 1972), thus indicating that a small percentage of H remains at these sites as shown in Table 11. The contamination by H may be due to an insufficient number of recrystallizations for complete exchange, or, more likely, it may indicate that the D_2O used in this study was impure. The difference in percentage of H between the D(4) and D(5) sites is significant judging from the e.s.d.'s.

The relationship between the H:D exchange ratio and hydrogen-bonding environment has been studied using nearly a null-matrix with respect to the H,D atoms in α-oxalic acid dihydrate (Coppens, 1970) and ammonium oxalate monohydrate (Taylor & Sabine, 1972). These studies indicate that the protons show a definite preference for the site which participates in the short O–H···O bond in oxalic acid, and for the water molecules relative to the ammonium ions in ammonium oxalate monohydrate. In a 50% deuterated sample of yttrium oxalate trihydrate, which contains an $H_5O_2^+$ ion and an additional water molecule that forms no hydrogen bonds, the protons are found to occupy preferentially the central position in the $H_5O_2^+$ ion (Brunton & Johnson, 1975). In deuterated decaborane a higher percentage of residual H was found at bridged, than at terminal positions (Tippe & Hamilton, 1969) while in a partially deuterated sample of $H_2Os_3(CO)_{10}CH_2$, the H was found to occupy preferentially the bridging osmium hydride positions and

the D the methylene-group sites (Calvert, Shapley, Schultz, Williams, Suib & Stucky, 1978). The proton occupancies for D-QNA given in Table 11 are in accord with the observations cited above, and with simple energy considerations, which imply that the D atoms should prefer the sites with deepest potential wells. It is tempting to speculate that the slightly more equal distribution of protons at 298 K compared to that at the lower temperatures may be due to an entropy contribution. A similar tendency toward more equal H:D ratios at higher temperatures was observed in yttrium oxalate trihydrate where the sensitivity was enhanced owing to the use of an overall D fraction of 0·5. However, in the present study this temperature-dependent effect lies at the 1σ level and is of marginal significance.

We wish to thank Joseph Henriques for technical assistance, and Philip Coppens, Franz Reidinger, and Jacques Verbist for helpful discussions.

References

ALCOCK, N. W. (1970). *Crystallographic Computing*, edited by F. R. AHMED, pp. 271–278. Copenhagen: Munksgaard.

BACON, G. E. (for NEUTRON DIFFRACTION COMMISSION) (1972). *Acta Cryst.* A**28**, 357–358.

BECKER, P. J. & COPPENS, P. (1975). *Acta Cryst.* A**31**, 417–425.

BRUNTON, G. D. & JOHNSON, C. K. (1975). *J. Chem. Phys.* **62**, 3797–3806.

BUSING, W. R., MARTIN, K. O. & LEVY, H. A. (1962). *ORFLS*. Report ORNL-TM-305. Oak Ridge National Laboratory, Tennessee.

CALVERT, R. B., SHAPLEY, J. R., SCHULTZ, A. J., WILLIAMS, J. M., SUIB, S. L. & STUCKY, G. D. (1978). *J. Am. Chem. Soc.* **100**, 6240–6241.

COPPENS, P. (1970). *Thermal Neutron Diffraction*, edited by B. T. M. WILLIS, pp. 82–100. Oxford Univ. Press.

DELAPLANE, R. G. & IBERS, J. A. (1969). *Acta Cryst.* B**25**, 2423–2437.

DIMMLER, D. G., GREENLAW, N., KELLEY, M. A., POTTER, D. W., RANKOWITZ, S. & STUBBLEFIELD, F. W. (1976). *IEEE Trans. Nucl. Sci.* NS-**23**, 398–405.

HAMILTON, W. C. (1965). *Acta Cryst.* **18**, 502–510.

JOHNSON, C. K. (1969). *Acta Cryst.* A**25**, 187–194.

JOHNSON, C. K. (1970*a*). Chemistry Division Annual Progress Report ORNL-4581, pp. 133–134. Oak Ridge National Laboratory, Tennessee.

JOHNSON, C. K. (1970*b*). *ORJFLS*. Unpublished work.

JOHNSON, C. K. (1976). *ORTEP*-II. Report ORNL-5138. Oak Ridge National Laboratory, Tennessee.

KOESTER, L (1977). *Neutron Physics*, edited by L. KOESTER & A. STEYERL, p. 36. Berlin, Heidelberg, New York: Springer.

KVICK, Å (1978). Private communication.

KVICK, Å., KOETZLE, T. F., THOMAS, R. & TAKUSAGAWA, F. (1974). *J. Chem. Phys.* **60**, 3866–3874.

MCMULLAN, R. K., ANDREWS, L. C., KOETZLE, T. F., REIDINGER, F., THOMAS, R. & WILLIAMS, G. J. B. (1976). *NEXDAS. Neutron and X-ray Data Acquisition System.* Unpublished work.

MEULENAER, J. DE & TOMPA, H. (1965). *Acta Cryst.* **19**, 1014–1018.

ROBERTSON, J. M. & UBBELOHDE, A. R. (1939). *Proc. R. Soc. London Ser. A*, **170**, 222–240, 241–251.

SCHOMAKER, V. & TRUEBLOOD, K. N. (1968). *Acta Cryst.* B**24**, 63–76.

SHULL, C. G. (1972). Private communication.

TAKUSAGAWA, F., HIROTSU, K. & SHIMADA, A. (1973). *Bull. Chem. Soc. Jpn*, **46**, 2372–2380.

TAKUSAGAWA, F. & KOETZLE, T. F. (1978). *Acta Cryst.* B**34**, 1149–1154.

TAYLOR, J. C. & SABINE, T. M. (1972). *Acta Cryst.* B**28**, 3340–3351.

TEMPLETON, D. H. & TEMPLETON, L. K. (1973). Am. Crystallogr. Assoc. Meeting, Storrs, Connecticut. Abstract E10.

THOMAS, J. O. (1972). *Acta Cryst.* B**28**, 2037–2045.

THOMAS, J. O., TELLGREN, R. & OLOVSSON, I. (1974). *Acta Cryst.* B**30**, 1155–1166.

TIPPE, A. & HAMILTON, W. C. (1969). *Inorg. Chem.* **8**, 464–470.

Acta Cryst. (1979). B**35**, 2135–2140

4-Octadecynoic Acid, a Largely Regular Structure in Space Group $P\bar{1}$

BY FRODE MO

Institutt for røntgenteknikk, Universitetet i Trondheim-NTH, N-7034 Trondheim-NTH, Norway

(*Received* 11 *April* 1979; *accepted* 21 *May* 1979)

Abstract

$C_{18}H_{32}O_2$ is triclinic ($P\bar{1}$) with $a = 8{\cdot}71\ (2)$, $b = 5{\cdot}475\ (10)$, $c = 45{\cdot}13\ (7)$ Å; $\alpha = 92{\cdot}55\ (15)$, $\beta = 93{\cdot}15\ (15)$, $\gamma = 123{\cdot}95\ (25)°$, $Z = 4$. The structure which has some OD character was solved in two discrete steps by direct and Patterson methods. Full-matrix least-squares refinement based on 1155 F_o from visually estimated film intensities was terminated at $R = 0{\cdot}071$. In the ordered structure, neighbouring

0567-7408/79/092135-06$01.00

© 1979 International Union of Crystallography